doi: 10.82124/CEAS-GNC-2026-056 CEAS-GNC-2026-056

Trajectory Prediction of Maneuverable Non-Cooperative Spacecraft Using Time-Series Diffusion Model

Haoqi Huang Ph.D Student, Harbin Institute of Technology, Department of Control Science and Engineering, 150001, Harbin, China. 25b304024@stu.hit.edu.cn

Pengyu Wang Professor, Harbin Institute of Technology, Department of Control Science and Engineering, 150001, Harbin, China. wangpy@hit.edu.cn

Yuhan Liu Associate Professor, Harbin Institute of Technology, Department of Control Science and Engineering, 150001, Harbin, China. yhliu@hit.edu.cn

Shaoming He Professor, Beijing Institute of Technology, School of Aerospace Engineering, 100081, Beijing, China. shaoming.he@bit.edu.cn

Yanning Guo Professor, Harbin Institute of Technology, Department of Control Science and Engineering, 150001, Harbin, China. guoyn@hit.edu.cn

ABSTRACT

Trajectory prediction of non-cooperative spacecraft constitutes an important component of space defense. Existing studies have primarily focused on configuration classification and parameter identification under the assumption that the motion conforms to a fixed configuration or that the control laws possess a known form, thereby enabling prediction of the future motion of non-cooperative spacecraft. In this paper, a diffusion-based time-series prediction model is introduced, which is not constrained by the aforementioned assumptions. A pursuit–evasion trajectory dataset is constructed in a representative close-range pursuit–evasion game scenario using reinforcement learning. The applicability of the Denoising Diffusion Probabilistic Model to the trajectory prediction task is then demonstrated. Finally, the effectiveness of the proposed model is validated through numerical simulations, in which comparisons with other time-series prediction models are presented, and model predictive control is subsequently employed to intercept the non-cooperative spacecraft based on the predicted trajectories.

Nomenclature

$\mathcal{S}$	=	A measurable state space, $\mathcal{S} \subseteq \mathbb{R}^d$
$\mathcal{A}$	=	A measurable action space
S_t	=	State at physical time t
A_t	=	Action at physical time t
$\pi(A \mid S)$	=	A stationary, possibly stochastic, policy $A_t \sim \pi(\cdot \mid S_t)$
$c_{t-m+1:t}$	=	The conditioning context, consisting of the last m states
$\tau_{t+1:t+n}$	=	The target n-step future state trajectory

$\mathbf{x}^{(0)}$	=	The flattened vector representation of $\tau_{t+1:t+n}$
$P(S' \mid S, A)$	=	The state transition kernel of the underlying MDP
$p_{\text{data}}(\cdot \mid c)$	=	The true conditional data distribution of $\tau_{t+1:t+n}$ given history c
$p_\theta(\cdot \mid c)$	=	The model's parameterized approximation of the data distribution
ϵ_θ	=	A neural network with parameters θ that predicts noise
$D_{\text{KL}}(p\|q)$	=	The Kullback–Leibler divergence
$\{\beta_k\}_{k=1}^K$	=	A fixed variance schedule for the diffusion process
$\alpha_k, \bar{\alpha}_k$	=	Derived parameters for the diffusion schedule, where $\alpha_k = 1 - \beta_k$ and $\bar{\alpha}_k = \prod_{j=1}^k \alpha_j$

1 Introduction

Within the framework of orbital game theory, accurate prediction for the motion behavior and trajectory of non-cooperative spacecraft is essential for supporting defensive and interceptive maneuvers. Existing studies generally classify the behavior of such spacecraft into two categories: motion constrained by a fixed orbital configuration, and maneuvering governed by an underlying control law or strategy. In the former case, the trajectory can be inferred by analyzing real-time and historical motion data according to the characteristics of the prescribed configuration. In the latter case, however, effective trajectory prediction requires first identifying the maneuvering strategy, which enables anticipation of subsequent maneuvers and future trajectory evolution.

For spacecraft constrained by prescribed orbital configurations, pioneer studies have classified motion patterns into categories such as rendezvous, circumnavigation, teardrop hovering, and drifting, according to their distinct orbital characteristics. To identify these patterns, sequence-learning methods including Bidirectional Gated Recurrent Unit with self-attention (BiGRU-self-attention [1]) and Deep Neural Networks (DNNs) [2] have been applied to real-time motion state sequences. Building upon previous work [2], Luo et al. [3] employed on-board optical imagery of real-time motion state as input to a Convolutional Neural Network (CNN) for configuration classification. Based on prior work, Sun et al. in [4] summarized 38 different motion configurations and demonstrated through experiments that the BiGRU-Attention classification model achieved the highest accuracy. More recently, Wang et al. [5] developed a method that assigns behavior weights to non-cooperative spacecraft across three situational functions: circumnavigation, collision, and observation. Their approach utilizes a meta-learning-based fuzzy decision tree integrated with Long-Short Term Memory (LSTM) spatio-temporal modeling and quantum genetic optimization. Chen et al. and Yang et al. in [6] and [7] also modeled the spacecraft behavior using membership functions, and then predicted future behavioral intentions through Bayesian inference or fuzzy decision trees. Nevertheless, these approaches above fundamentally rely on predefined intention categories, which limit their ability to anticipate the future actions of a non-cooperative spacecraft and to guide the defender's subsequent evasion and interception maneuvers.

Beyond configuration-based classification, a main challenge arises when spacecraft engage in game-theoretic maneuvers governed by a fixed strategy, where the primary task is to learn the underlying strategy. Currently, strategy generation is mainly based on either differential game theory [8–13] or deep reinforcement learning [14–16]. Among these, strategies derived from typical quadratic differential games have attracted particular attention due to their explicit mathematical formulation and high interpretability. A common assumption in existing works is that the non-cooperative spacecraft employs quadratic optimal control with a known objective function. Under this assumption, the aforementioned strategy identification problem can be transformed into an online parameter estimation task. For instance, Li et al. [17] utilized an Improved Strong Tracking Unscented Kalman Filter (ISTUKF) to estimate the pursuer's game parameters in real time, thereby refining parameter estimates and updating the evasion strategy throughout the engagement. To address the case of an unknown cost matrix, Ye et al. [18] and Tang et al. [19] adopted different filtering-based methods to construct adaptive estimators and controllers,

which then informed their respective interception strategies. However, these approaches are inherently tied to the quadratic optimal control assumption, and their applicability is significantly limited when the non-cooperative spacecraft utilizes more general or non-optimal maneuvering strategies.

As noted in aforementioned research, existing studies still lack effective trajectory prediction methods for maneuverable non-cooperative spacecraft whose control laws neither maintain a fixed configuration nor conform to a specific predefined structure. To address this gap, we propose a time-series prediction approach. In particular, we first construct a trajectory dataset based on a pursuit-evasion strategy derived from a reinforcement learning policy that is not explicitly identifiable. Subsequently, a Denoising Diffusion Probabilistic Model (DDPM) is trained on the designated training set extracted from the dataset to forecast the future trajectories of the non-cooperative spacecraft using its historical motion data. Finally, the predicted trajectories are employed as nominal guidance for the interceptor spacecraft within a model predictive control (MPC) framework to execute the interception task under given constraints.

The remainder of this paper is organized as follows. In Section 2, a pursuit–evasion game scenario involving three spacecraft is established, and the corresponding dynamics are presented. In Section 3, the principles of DDPM are described in detail, and its applicability to the trajectory prediction problem of non-cooperative spacecraft is demonstrated. In Section 4, simulation validation of trajectory prediction using DDPM is provided, and MPC-based interception is performed based on the predicted trajectories.

2 Problem Statement

In this section, we investigates the close-proximity pursuit-evasion problem of spacecraft, modeled by the CW equations. As shown in Fig. 1, the pursuer P aims to minimize its distance from the evader E, while the evader seeks to maximize this distance. Furthermore, a defender D is introduced to protect the evader E. Even though the defender D does not directly engage in the pursuit-evasion game, it is required to maintain its trajectory overlap with the pursuer P for as long as possible, thereby providing sufficient time to operate on or destroy P. The pursuer is modeled as a non-cooperative target, and the primary objective of this work is to predict its trajectory and enable the defender to perform a rapid interception.

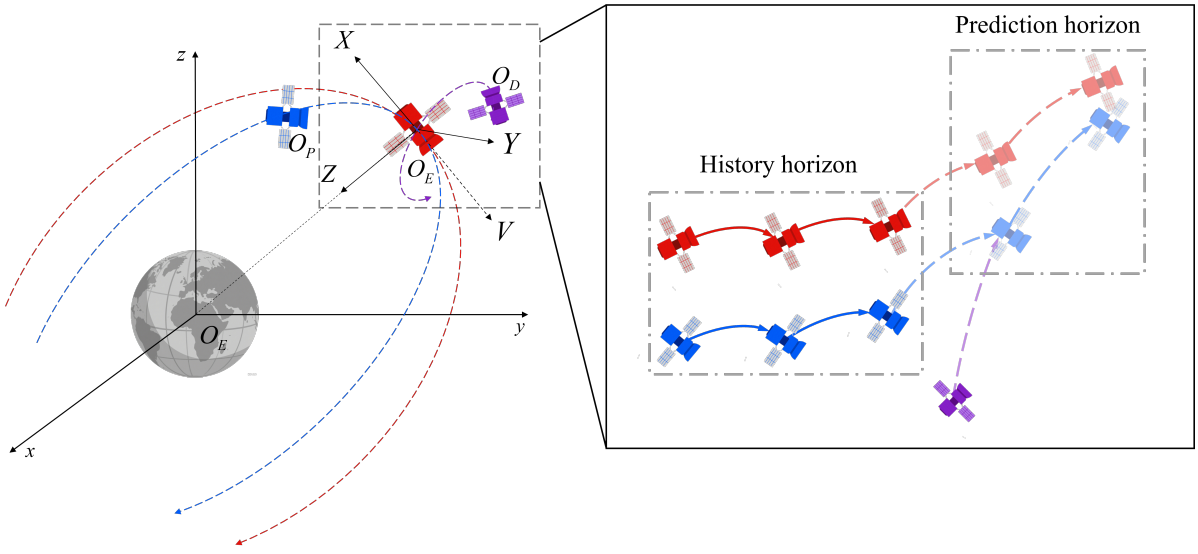

Fig. 1 Illustration of the key elements in a two-player orbital game, detailing both the scenario dynamics and the objective of the trajectory prediction task.

The position and velocity of spacecraft are described by a six-dimensional vector $\boldsymbol{p}_i = [x, y, z, v_x, v_y, v_z]^\top$. Throughout the entire game, the position and velocity of all spacecraft are observable. The distances among the three spacecrafts E, D, and P during the game are set to be within 300 km. Since this satisfies the Clohessy-Wiltshire (CW) dynamics requirement that relative distances are much smaller than the

orbital radius, this paper uses CW equations in the Hill coordinate system to describe the motion of the three spacecrafts (1).

$$\begin{cases} \ddot{x} - 2\omega\dot{z} = u_x \\ \ddot{y} + \omega^2 y = u_y \\ \ddot{z} + 2\omega\dot{x} - 3\omega^2 z = u_z \end{cases} \tag{1}$$

The origin of the Hill coordinate system is located at the initial position of spacecraft E and orbits the Earth without maneuver. Under the assumption of fixed-interval impulsive thrust, the equation of motion for the three-spacecraft in three-dimensional Hill coordinate system can be expressed in the following compact form:

$$\begin{gathered} \dot{\boldsymbol{p}} = \boldsymbol{A}\boldsymbol{p} + \boldsymbol{B}\boldsymbol{u}, \boldsymbol{y} = \boldsymbol{C}\boldsymbol{p}, \boldsymbol{p} = [x, y, z, \dot{x}, \dot{y}, \dot{z}]^\top, \boldsymbol{u} = [u_x, u_y, u_z]^\top \\ \boldsymbol{A} = \begin{bmatrix} 0 & 0 & 0 & 1 & 0 & 0 \\ 0 & 0 & 0 & 0 & 1 & 0 \\ 0 & 0 & 0 & 0 & 0 & 1 \\ 0 & 0 & 0 & 0 & 2\omega & 0 \\ 0 & 3\omega^2 & 0 & -2\omega & 0 & 0 \\ 0 & 0 & -\omega^3 & 0 & 0 & 0 \end{bmatrix}, \boldsymbol{B} = \begin{bmatrix} 0 & 0 & 0 \\ 0 & 0 & 0 \\ 0 & 0 & 0 \\ 1 & 0 & 0 \\ 0 & 1 & 0 \\ 0 & 0 & 1 \end{bmatrix}, \boldsymbol{C} = \begin{bmatrix} 1 & 0 & 0 & 0 & 0 & 0 \\ 0 & 1 & 0 & 0 & 0 & 0 \\ 0 & 0 & 1 & 0 & 0 & 0 \\ 0 & 0 & 0 & 1 & 0 & 0 \\ 0 & 0 & 0 & 0 & 1 & 0 \\ 0 & 0 & 0 & 0 & 0 & 1 \end{bmatrix} \end{gathered} \tag{2}$$

where ω is the orbital angular velocity, the solution of (2) can be obtained as:

$$\begin{gathered} \boldsymbol{p}_t = \boldsymbol{\Phi}(t, t_0)\, \boldsymbol{p}_0 + \int_{t_0}^{t} \boldsymbol{\Phi}_v(t, \tau)\, \boldsymbol{B}\boldsymbol{u}(\tau)\, d\tau \\ \tau = t - t_0, c = \cos\omega\tau, s = \sin\omega\tau \\ \Phi(t, t_0) = \begin{bmatrix} 1 & 0 & 6(\tau - s) & \frac{(4s-3\tau)}{\omega} & 0 & \frac{2(1-c)}{\omega} \\ 0 & c & 0 & 0 & \frac{s}{\omega} & 0 \\ 0 & 0 & 4 - 3c & \frac{2(c-1)}{\omega} & 0 & \frac{s}{\omega} \\ 0 & 0 & 6\omega(1-c) & 4c - 3 & 0 & 2s \\ 0 & -\omega s & 0 & 0 & c & 0 \\ 0 & 0 & 3\omega s & -2s & 0 & c \end{bmatrix} \end{gathered} \tag{3}$$

According to the assumption of fixed-interval impulsive thrust, the integral term in (3) can be eliminated. Thus, the solution to the state equation can be simplified as (4) .

$$\begin{aligned} \boldsymbol{p}(t) &= \boldsymbol{\Phi}(t, t_0)\, \boldsymbol{p}(t_0^+) \\ \boldsymbol{p}(t_0^+) &= [x(t_0^-), y(t_0^-), z(t_0^-), \left(\boldsymbol{v}(t_0^-) + \Delta\boldsymbol{V}(t_0)\right)^\top]^\top \end{aligned} \tag{4}$$

In this paper, we assume that the pursuer P follows a pursuit policy obtained through multi-stage self-play reinforcement learning, together with the impulsive dynamics described in (4). Within this self-play framework, the opponent acts as an evader driven by a reinforcement learning strategy with a contrary objective. The pursuer P subsequently applies the learned pursuit strategy against evaders adopting diverse tactics, thereby producing a trajectory dataset.

3 Method

In this section, we first present the definitions of the spacecraft decision-making process under the Markov assumption, along with the time-series denoising diffusion probabilistic model (DDPM, [20]). Subsequently, we rigorously demonstrate the applicability of the time-series diffusion model for predicting the trajectory of a spacecraft operating under a fixed policy.

3.1 Definitions of Decision Process and Diffusion Model

Assuming that the decision-making process of the spacecraft satisfies the Markov property, if we aim to predict its future trajectory based on historical motion data, namely to estimate the conditional distribution $p_{\text{data}}(\tau_{t+1:t+n} \mid c_{t-m+1:t})$, then in a Markov Decision Process governed by a policy π, this distribution can be obtained by marginalizing over the future action sequence $A_t, \ldots, A_{t+n-1}$. We therefore provide the relevant definitions to describe the spacecraft's decision-making process, and present the fundamental principles and derivations of the time-series diffusion model.

Definition 3.1 (True Future Trajectory Distribution)**.** Given the history $c_{t-m+1:t}$, the distribution of the future state trajectory $\tau_{t+1:t+n}$ is:

$$p_{\text{data}}(\tau_{t+1:t+n} \mid c_{t-m+1:t}) = \int \cdots \int \left[\prod_{j=0}^{n-1} P(S_{t+j+1} \mid S_{t+j}, A_{t+j})\, \pi(A_{t+j} \mid S_{t+j}) \right] dA_t \ldots dA_{t+n-1}. \quad (5)$$

Definition 3.2 (Forward Diffusion Process)**.** The forward process q is a Markov chain that gradually adds Gaussian noise to a data vector $\mathbf{x}^{(0)}$ (the flattened trajectory) over K diffusion steps:

$$q(\mathbf{x}^{(k)} \mid \mathbf{x}^{(k-1)}) = \mathcal{N}\left(\mathbf{x}^{(k)}; \sqrt{\alpha_k}\mathbf{x}^{(k-1)}, \beta_k \mathbf{I}\right). \quad (6)$$

This process has a closed-form solution for sampling at any diffusion step k:

$$q(\mathbf{x}^{(k)} \mid \mathbf{x}^{(0)}) = \mathcal{N}\left(\mathbf{x}^{(k)}; \sqrt{\bar{\alpha}_k}\mathbf{x}^{(0)}, (1-\bar{\alpha}_k)\mathbf{I}\right). \quad (7)$$

Definition 3.3 (Conditional Reverse Process)**.** The reverse process p_θ learns to denoise, starting from pure noise $\mathbf{x}^{(K)} \sim \mathcal{N}(0, \mathbf{I})$ and progressively generating data conditioned on the history c. It is defined as a Markov chain parameterized by θ:

$$p_\theta(\mathbf{x}^{(0:K)} \mid c) = p(\mathbf{x}^{(K)}) \prod_{k=K}^{1} p_\theta(\mathbf{x}^{(k-1)} \mid \mathbf{x}^{(k)}, c), \quad (8)$$

where each reverse step is a Gaussian whose mean is predicted by the network ϵ_θ:

$$p_\theta(\mathbf{x}^{(k-1)} \mid \mathbf{x}^{(k)}, c) = \mathcal{N}\left(\mathbf{x}^{(k-1)}; \boldsymbol{\mu}_\theta(\mathbf{x}^{(k)}, k, c), \tilde{\beta}_k \mathbf{I}\right). \quad (9)$$

The mean and variance are given by:

$$\boldsymbol{\mu}_\theta(\mathbf{x}^{(k)}, k, c) = \frac{1}{\sqrt{\alpha_k}}\left(\mathbf{x}^{(k)} - \frac{\beta_k}{\sqrt{1-\bar{\alpha}_k}}\epsilon_\theta(\mathbf{x}^{(k)}, k, c)\right), \quad (10)$$

$$\tilde{\beta}_k = \frac{1-\bar{\alpha}_{k-1}}{1-\bar{\alpha}_k}\beta_k. \quad (11)$$

Derivation of (7) We derive the expression for $q(\mathbf{x}^{(k)} \mid \mathbf{x}^{(0)})$ by recursively expanding the one-step definition. Let $\mathbf{z}_j \sim \mathcal{N}(0, \mathbf{I})$ be i.i.d. standard Gaussian noise.

One-step process:

$$\mathbf{x}^{(k)} = \sqrt{\alpha_k}\mathbf{x}^{(k-1)} + \sqrt{\beta_k}\mathbf{z}_{k-1}. \tag{12}$$

Recursive expansion:

$$\begin{aligned}\mathbf{x}^{(k)} &= \sqrt{\alpha_k}\left(\sqrt{\alpha_{k-1}}\mathbf{x}^{(k-2)} + \sqrt{\beta_{k-1}}\mathbf{z}_{k-2}\right) + \sqrt{\beta_k}\mathbf{z}_{k-1} \\ &= \sqrt{\alpha_k\alpha_{k-1}}\mathbf{x}^{(k-2)} + \sqrt{\alpha_k\beta_{k-1}}\mathbf{z}_{k-2} + \sqrt{\beta_k}\mathbf{z}_{k-1} \\ &\quad \dots\end{aligned} \tag{13}$$

Using $\bar{\alpha}_k = \prod_{j=1}^{k} \alpha_j$, we get:

$$\mathbf{x}^{(k)} = \sqrt{\bar{\alpha}_k}\mathbf{x}^{(0)} + \text{noise}. \tag{14}$$

Variance summation:

The variance of the aggregated noise is:

$$\text{Var} = (\alpha_k \dots \alpha_2)\beta_1 + (\alpha_k \dots \alpha_3)\beta_2 + \dots + \alpha_k\beta_{k-1} + \beta_k, \tag{15}$$

which telescopes to:

$$1 - \bar{\alpha}_k. \tag{16}$$

Conclusion:

Combining (14) and (16) yields the closed form (7). □

Derivation of (10) **and** (11) From Definition 3.2, we have:

$$q(\mathbf{x}^{(k)} \mid \mathbf{x}^{(0)}) = \mathcal{N}\left(\sqrt{\bar{\alpha}_k}\mathbf{x}^{(0)}, (1 - \bar{\alpha}_k)\mathbf{I}\right), \tag{17}$$

$$q(\mathbf{x}^{(k-1)} \mid \mathbf{x}^{(0)}) = \mathcal{N}\left(\sqrt{\bar{\alpha}_{k-1}}\mathbf{x}^{(0)}, (1 - \bar{\alpha}_{k-1})\mathbf{I}\right). \tag{18}$$

The joint distribution of $(\mathbf{x}^{(k-1)}, \mathbf{x}^{(k)})$ given $\mathbf{x}^{(0)}$ is:

$$\begin{pmatrix}\mathbf{x}^{(k-1)} \\ \mathbf{x}^{(k)}\end{pmatrix} \sim \mathcal{N}\left(\begin{pmatrix}\sqrt{\bar{\alpha}_{k-1}}\mathbf{x}^{(0)} \\ \sqrt{\bar{\alpha}_k}\mathbf{x}^{(0)}\end{pmatrix}, \begin{pmatrix}(1 - \bar{\alpha}_{k-1})\mathbf{I} & \sqrt{\alpha_k}(1 - \bar{\alpha}_{k-1})\mathbf{I} \\ \sqrt{\alpha_k}(1 - \bar{\alpha}_{k-1})\mathbf{I} & (1 - \bar{\alpha}_k)\mathbf{I}\end{pmatrix}\right). \tag{19}$$

Applying the conditional Gaussian formula gives the variance:

$$\tilde{\beta}_k = \frac{1 - \bar{\alpha}_{k-1}}{1 - \bar{\alpha}_k}\beta_k, \tag{20}$$

and the mean:

$$\boldsymbol{\mu}_q(\mathbf{x}^{(k)}, \mathbf{x}^{(0)}) = \sqrt{\bar{\alpha}_{k-1}}\mathbf{x}^{(0)} + \frac{\sqrt{\alpha_k}(1 - \bar{\alpha}_{k-1})}{1 - \bar{\alpha}_k}\left(\mathbf{x}^{(k)} - \sqrt{\bar{\alpha}_k}\mathbf{x}^{(0)}\right). \tag{21}$$

Reparameterizing $\mathbf{x}^{(0)}$ in terms of $\mathbf{x}^{(k)}$ and noise $\boldsymbol{\epsilon}$:

$$\mathbf{x}^{(0)} = \frac{\mathbf{x}^{(k)} - \sqrt{1-\bar{\alpha}_k}\,\boldsymbol{\epsilon}}{\sqrt{\bar{\alpha}_k}}, \tag{22}$$

and substituting the approximation from ϵ_θ yields:

$$\boldsymbol{\mu}_\theta(\mathbf{x}^{(k)}, k, c) = \frac{1}{\sqrt{\alpha_k}}\left(\mathbf{x}^{(k)} - \frac{\beta_k}{\sqrt{1-\bar{\alpha}_k}}\,\epsilon_\theta(\mathbf{x}^{(k)}, k, c)\right), \tag{23}$$

which is (10). The reverse step is thus (9) with variance (20). □

3.2 Applicability Proof of the Diffusion Model

Lemma 3.1 (Conditional Sufficiency of m-step History)**.** *In an MDP with policy $\pi(A|S)$, the distribution of the future trajectory $\tau_{t+1:t+n}$ depends on the entire history $\mathcal{H}_t = (\ldots, S_t)$ only through the last m states $c_{t-m+1:t}$:*

$$p_{\text{data}}(\tau_{t+1:t+n} \mid \mathcal{H}_t) = p_{\text{data}}(\tau_{t+1:t+n} \mid c_{t-m+1:t}). \tag{24}$$

Proof. By the chain rule of probability, the joint density of future states and actions given $\mathcal{H}_t$ can be factorized, using the Markov property and the stationary policy:

$$\begin{aligned} &p(\tau_{t+1:t+n}, A_t, \ldots, A_{t+n-1} \mid \mathcal{H}_t) \\ &\quad = \prod_{j=0}^{n-1} P(S_{t+j+1} \mid S_{t+j}, A_{t+j}) \cdot \pi(A_{t+j} \mid S_{t+j}). \end{aligned} \tag{25}$$

From (25), the only state from the history $\mathcal{H}_t$ that appears is S_t (in the term for $j = 0$). All other states S_{t+j} for $j > 0$ are part of the future trajectory being modeled. Therefore, integrating (25) over actions yields a conditional distribution depending only on S_t from the context $c_{t-m+1:t}$:

$$p_{\text{data}}(\tau_{t+1:t+n} \mid \mathcal{H}_t) = p_{\text{data}}(\tau_{t+1:t+n} \mid S_t) = p_{\text{data}}(\tau_{t+1:t+n} \mid c_{t-m+1:t}), \tag{26}$$

which matches the sufficiency statement in (24). □

Lemma 3.2 (Trajectory-Vector Isomorphism)**.** *If the state space $\mathcal{S} \subset \mathbb{R}^d$ is a Borel set, the flattening map $f : \mathcal{S}^n \to \mathbb{R}^{dn}$, defined by $f(s_1, \ldots, s_n) = (s_1^\top, \ldots, s_n^\top)^\top$, is a Borel isomorphism that preserves KL divergence. That is, for any pair of probability densities p, q on $\mathcal{S}^n$, letting their induced densities on $\mathbb{R}^{dn}$ via f be p', q', it holds that:*

$$D_{\text{KL}}(p\|q) = D_{\text{KL}}(p'\|q'). \tag{27}$$

Proof. The definition of KL divergence is:

$$D_{\text{KL}}(p\|q) := \int_{\mathcal{S}^n} p(\tau) \log \frac{p(\tau)}{q(\tau)}\, d\tau. \tag{28}$$

We perform a change of variables, letting $\tau = f^{-1}(\mathbf{x})$, where $\mathbf{x} \in \mathbb{R}^{dn}$. The map f is a linear bijection, thus its inverse f^{-1} is also linear. The Jacobian of this transformation, $J_{f^{-1}}(\mathbf{x})$, is a constant matrix. Since f is merely a reordering and concatenation operation, the absolute value of its Jacobian determinant is:

$$|\det(J_{f^{-1}}(\mathbf{x}))| = 1. \tag{29}$$

By the change of variables formula for probability densities, the induced densities $p'(\mathbf{x})$ and $q'(\mathbf{x})$ satisfy:

$$p'(\mathbf{x}) = p(f^{-1}(\mathbf{x}))\,|\det(J_{f^{-1}}(\mathbf{x}))| = p(f^{-1}(\mathbf{x})), \tag{30}$$

$$q'(\mathbf{x}) = q(f^{-1}(\mathbf{x}))\,|\det(J_{f^{-1}}(\mathbf{x}))| = q(f^{-1}(\mathbf{x})). \tag{31}$$

Substituting (30) and (31) into (28), and using (29), we have:

$$\begin{aligned} D_{\mathrm{KL}}(p\|q) &= \int_{\mathbb{R}^{dn}} p(f^{-1}(\mathbf{x})) \log \frac{p(f^{-1}(\mathbf{x}))}{q(f^{-1}(\mathbf{x}))}\,|\det(J_{f^{-1}}(\mathbf{x}))|\,d\mathbf{x} \\ &= \int_{\mathbb{R}^{dn}} p'(\mathbf{x}) \log \frac{p'(\mathbf{x})}{q'(\mathbf{x})} \cdot 1\,d\mathbf{x} \\ &\equiv D_{\mathrm{KL}}(p'\|q'). \end{aligned} \tag{32}$$

Therefore, the isomorphism preserves the KL divergence as stated in (27). □

Lemma 3.3 (Universality of Conditional DDPM)**.** *Assume the noise predictor $\epsilon_\theta(\mathbf{x}^{(k)}, k, c)$ is a universal function approximator. Then for any $\epsilon > 0$, there exists a parameter set θ^* such that the diffusion model p_{θ^*} constructed with this network satisfies:*

$$\sup_c D_{\mathrm{KL}}\big(q(\mathbf{x}^{(0)} \mid c) \,\|\, p_{\theta^*}(\mathbf{x}^{(0)} \mid c)\big) < \epsilon. \tag{33}$$

Here, $q(\mathbf{x}^{(0)} \mid c)$ represents the true (vectorized) conditional data distribution.

Proof. The Variational Lower Bound (VLB) of the diffusion model provides the following upper bound:

$$D_{\mathrm{KL}}\big(q(\mathbf{x}^{(0)}|c) \,\|\, p_\theta(\mathbf{x}^{(0)}|c)\big) \le \mathbb{E}_{q(\mathbf{x}^{(0:K)}|c)}\left[\sum_{k=2}^{K} L_k + L_0 + L_T\right], \tag{34}$$

where:

$$L_k := D_{\mathrm{KL}}\Big(q(\mathbf{x}^{(k-1)}|\mathbf{x}^{(k)}, \mathbf{x}^{(0)}) \,\|\, p_\theta(\mathbf{x}^{(k-1)}|\mathbf{x}^{(k)}, c)\Big), \quad k \ge 2, \tag{35}$$

$$L_0 := D_{\mathrm{KL}}\Big(q(\mathbf{x}^{(0)}|\mathbf{x}^{(1)}) \,\|\, p_\theta(\mathbf{x}^{(0)}|\mathbf{x}^{(1)}, c)\Big), \tag{36}$$

$$L_T := D_{\mathrm{KL}}\Big(q(\mathbf{x}^{(K)}|c) \,\|\, p(\mathbf{x}^{(K)})\Big), \tag{37}$$

with L_T representing the KL between the terminal forward distribution and the prior $p(\mathbf{x}^{(K)})$, L_0 the reconstruction term at $k = 1$, and L_k $(k \ge 2)$ the per-step KL terms along the reverse chain.

For $k \ge 2$, both $q(\mathbf{x}^{(k-1)}|\mathbf{x}^{(k)}, \mathbf{x}^{(0)})$ and $p_\theta(\mathbf{x}^{(k-1)}|\mathbf{x}^{(k)}, c)$ are Gaussian with identical covariance $\tilde{\beta}_k \mathbf{I}$. The KL between same-covariance Gaussians $\mathcal{N}(\mu_q, \Sigma)$ and $\mathcal{N}(\mu_\theta, \Sigma)$ reduces to:

$$D_{\mathrm{KL}}(\mathcal{N}(\mu_q, \Sigma) \,\|\, \mathcal{N}(\mu_\theta, \Sigma)) = \frac{1}{2}(\mu_q - \mu_\theta)^\top \Sigma^{-1} (\mu_q - \mu_\theta). \tag{38}$$

Here this yields:

$$L_k = \frac{1}{2\tilde{\beta}_k} \|\boldsymbol{\mu}_q(\mathbf{x}^{(k)}, \mathbf{x}^{(0)}) - \boldsymbol{\mu}_\theta(\mathbf{x}^{(k)}, c)\|^2. \tag{39}$$

The forward posterior mean is:

$$\boldsymbol{\mu}_q = \frac{1}{\sqrt{\alpha_k}} \left(\mathbf{x}^{(k)} - \frac{\beta_k}{\sqrt{1 - \bar{\alpha}_k}} \boldsymbol{\epsilon}\right), \tag{40}$$

and the reverse mean is:

$$\boldsymbol{\mu}_\theta = \frac{1}{\sqrt{\alpha_k}} \left(\mathbf{x}^{(k)} - \frac{\beta_k}{\sqrt{1-\bar{\alpha}_k}} \epsilon_\theta(\mathbf{x}^{(k)}, k, c) \right). \tag{41}$$

Subtracting (41) from (40) gives:

$$\boldsymbol{\mu}_q - \boldsymbol{\mu}_\theta = -\frac{\beta_k}{\sqrt{\alpha_k(1-\bar{\alpha}_k)}} \left[\epsilon_\theta(\mathbf{x}^{(k)}, k, c) - \boldsymbol{\epsilon} \right], \tag{42}$$

which substituted into (39) yields:

$$L_k = \frac{\beta_k^2}{2\alpha_k(1-\bar{\alpha}_k)\tilde{\beta}_k} \|\epsilon_\theta(\mathbf{x}^{(k)}, k, c) - \boldsymbol{\epsilon}\|^2. \tag{43}$$

For L_0, the same quadratic structure appears but with its own coefficient C_1, and L_T is constant with respect to θ given a fixed prior.

Defining:

$$C_k := \frac{\beta_k^2}{2\alpha_k(1-\bar{\alpha}_k)\tilde{\beta}_k}, \quad 1 \le k \le K, \tag{44}$$

we can rewrite (34) as:

$$D_{\mathrm{KL}}(q \,\|\, p_{\theta^*}) \le \sum_{k=1}^{K} C_k \, \mathbb{E}[\|\epsilon_{\theta^*} - \boldsymbol{\epsilon}\|^2] + \text{const.} \tag{45}$$

If ϵ_θ is a universal approximator, for any $\delta > 0$ there exists θ^* such that $\mathbb{E}[\|\epsilon_{\theta^*} - \boldsymbol{\epsilon}\|^2] < \delta$ for all k, c. Then:

$$D_{\mathrm{KL}}(q \,\|\, p_{\theta^*}) \le \left(\sum_{k=1}^{K} C_k \right) \delta + \text{const.} \tag{46}$$

Since $\sum_{k=1}^{K} C_k$ is finite, choosing δ sufficiently small ensures (33) holds. □

Theorem 3.4 (Universal Approximation of Trajectory Distributions)**.** *In an MDP with a stationary policy π, given a Borel state space and a universal approximator ϵ_θ, for any prediction horizon n, history length m, and precision $\epsilon > 0$, there exists a conditional DDPM with parameters θ^* such that:*

$$\sup_{c \in \mathcal{S}^m} D_{\mathrm{KL}} \left(p_{\mathrm{data}}(\tau_{t+1:t+n} \mid c) \,\|\, p_{\theta^*}(\tau_{t+1:t+n} \mid c) \right) < \epsilon. \tag{47}$$

Proof. We aim to demonstrate that the left-hand side of the expression can be rendered arbitrarily small. The proof is outlined as follows:

$$\begin{aligned}
&\sup_{c \in \mathcal{S}^m} D_{\mathrm{KL}} \left(p_{\mathrm{data}}(\tau_{t+1:t+n} \mid c) \,\|\, p_{\theta^*}(\tau_{t+1:t+n} \mid c) \right) \\
&= \sup_{c \in \mathcal{S}^m} D_{\mathrm{KL}} \left(f_\# p_{\mathrm{data}}(\cdot \mid c) \,\|\, f_\# p_{\theta^*}(\cdot \mid c) \right) \quad \text{(by Lemma 3.2, KL div. is invariant under isomorphism } f\text{)} \\
&= \sup_{c \in \mathcal{S}^m} D_{\mathrm{KL}} \left(q(\mathbf{x}^{(0)} \mid c) \,\|\, p'_{\theta^*}(\mathbf{x}^{(0)} \mid c) \right) \quad \text{(defining vectorized distributions as } q(\mathbf{x}^{(0)}|c) \text{ and } p'_{\theta^*}\text{)} \\
&< \epsilon. \quad \text{(by Lemma 3.3, for any } \epsilon > 0, \text{ there exists } \theta^* \\
&\qquad \text{such that the approximation error of model } p'_{\theta^*} \text{ to } q \text{ is less than } \epsilon\text{)}
\end{aligned}$$

Step 1: By Lemma 3.2 (Trajectory-Vector Isomorphism), we equivalently transform the KL divergence in the trajectory space ($\mathcal{S}^n$) to the KL divergence in the vector space ($\mathbb{R}^{dn}$).

Step 2: We rename the distributions in the vector space to match the notation of Lemma 3.3. The true trajectory distribution p_{data} is mapped by f to the true vector distribution q. Our model p_{θ^*} is itself defined in the vector space, so its distribution in this space is p'_{θ^*}.

Step 3: Lemma 3.3 (Universality of Conditional DDPM) proves that as long as ϵ_θ is a universal approximator, we can always find a set of parameters θ^* such that the KL divergence between the model distribution p'_{θ^*} and any true vector distribution q is less than any given positive number ϵ.

In summary, through the equivalence transformation and the universal approximation guarantee, we have shown that the KL divergence in the trajectory space can be controlled to be less than any arbitrarily small ϵ. □

4 Simulations

In this section, the prediction performance of the time-series forecasting DDPM described in Section 3 is presented on the trajectory dataset described in Section 2. From this trajectory dataset, a sliding-window sampling method is applied to construct the training and test sets for the trajectory prediction model.

Table 1 Predictive Performance of the GPR Model in [21]

Metric	Value
Average MSE	28.9671
Average MAE	3.8538
Average Euclidean Distance	7.7289
Average fitness%	66.89

Table 2 Predictive Performance of the Proposed Diffusion Model with MLP Noise-Fitting Network

Metric	Value
Average MSE	33.5562
Average MAE	4.0419
Average Euclidean Distance	8.1064
Average fitness%	65.92

Table 3 Predictive Performance of the Proposed Diffusion Model with Self-Attention Encoder

Metric	Value
Average MSE	12.7760
Average MAE	2.5653
Average Euclidean Distance	5.1382
Average fitness%	78.74

Figure 2 illustrates the prediction results of the model for three randomly selected historical trajectories from the test set. For performance comparison, we employ Gaussian process regression (GPR,[21]), Interacting multiple model (IMM) and DDPMs constructed with different types of noise-fitting networks. Simulation results indicate that the DDPM utilizing a self-attention encoder as the noise-fitting network

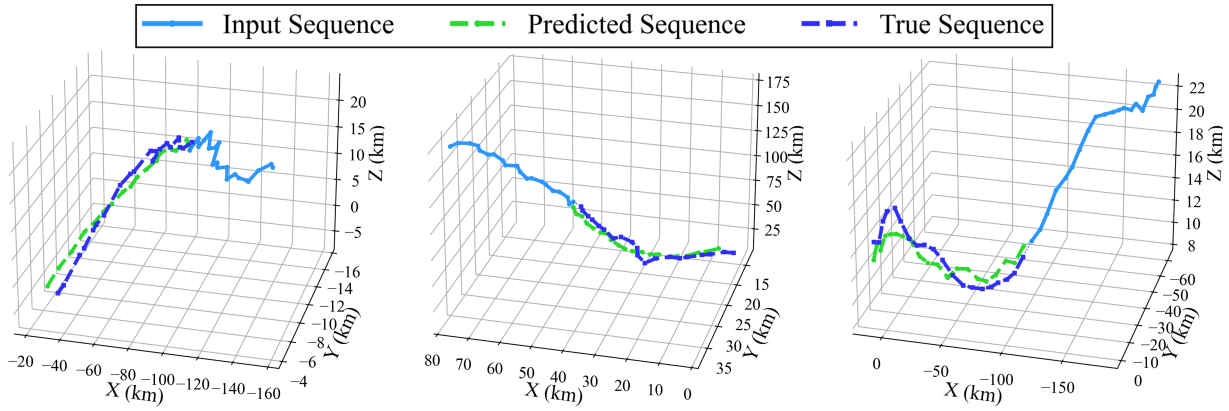

(a) Self-Attention Diffusion Model Prediction Result

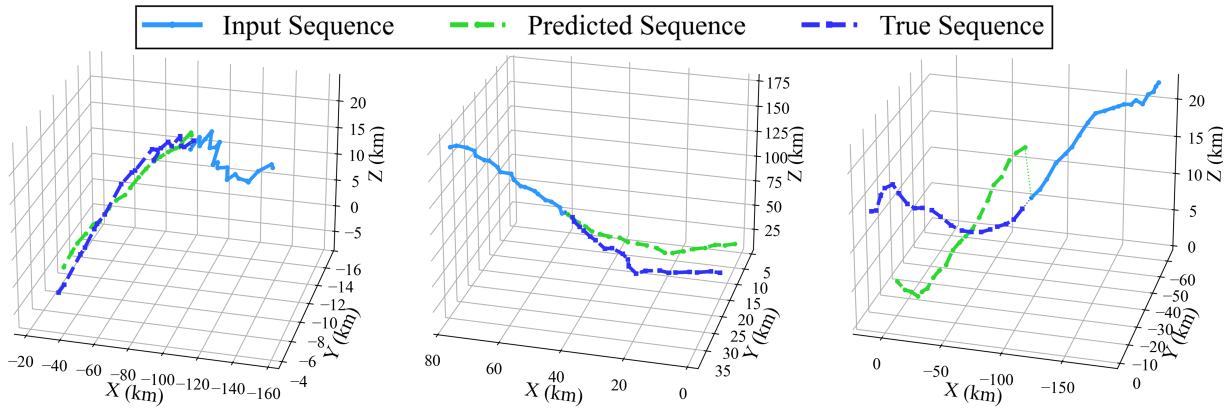

(b) Gaussian Process Regression Model Prediction Result

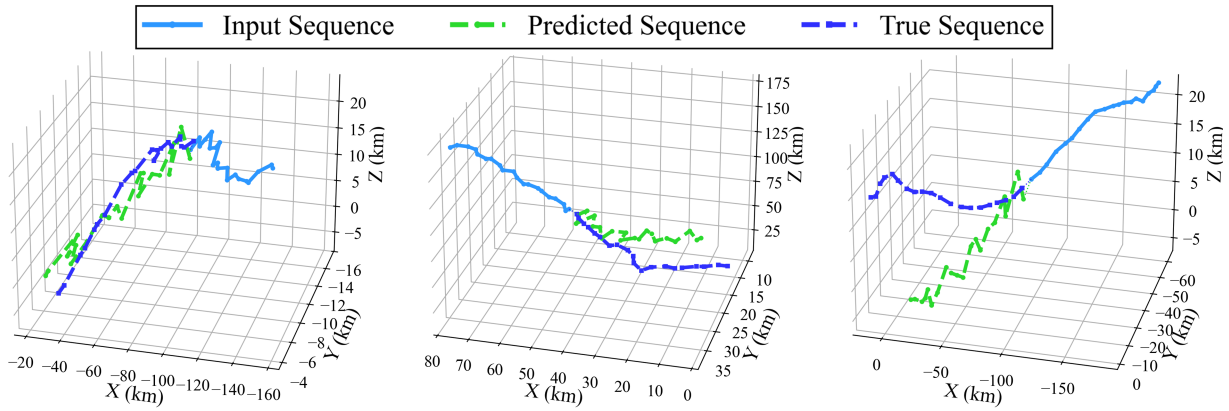

(c) MLP Diffusion Model Prediction Result

Fig. 2 A comparison of 20-step trajectory prediction results from different models, where the task is to forecast from a 20-step history, clearly highlighting the superior performance of the self-attention encoder-based diffusion model over the two alternative methods.

Table 4 Predictive Performance of the Interacting Multiple Model

Metric	Value
Average MSE	163.8136
Average MAE	7.9931
Average Euclidean Distance	15.947606
Average fitness%	40.03

achieves the best prediction performance, followed by GPR, while the IMM performs the worst. Table 1,2,4 and 3 summarizes the performance of these three prediction models over 1000 prediction trials, showing consistency with the results on the randomly selected trajectories. The definition of fitness% is given in (48):

$$\text{fit\%} = 100\left(1 - \frac{\|\widehat{\boldsymbol{s}}_{0:T-1} - \tilde{\boldsymbol{s}}_{0:T-1}\|_2}{\|\widehat{\boldsymbol{s}}_{0:T-1} - \bar{\boldsymbol{s}}\|_2}\right), \quad \bar{\boldsymbol{s}} \doteq \frac{1}{T}\sum_{k=0}^{T-1} \tilde{\boldsymbol{s}}_k \tag{48}$$

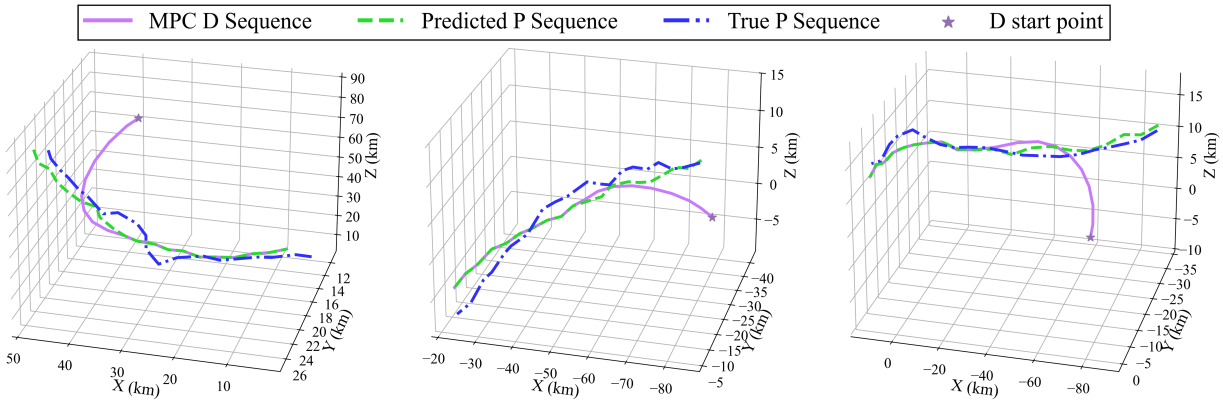

Fig. 3 Interception Trajectories under MPC with Self-Attention Diffusion Model Prediction

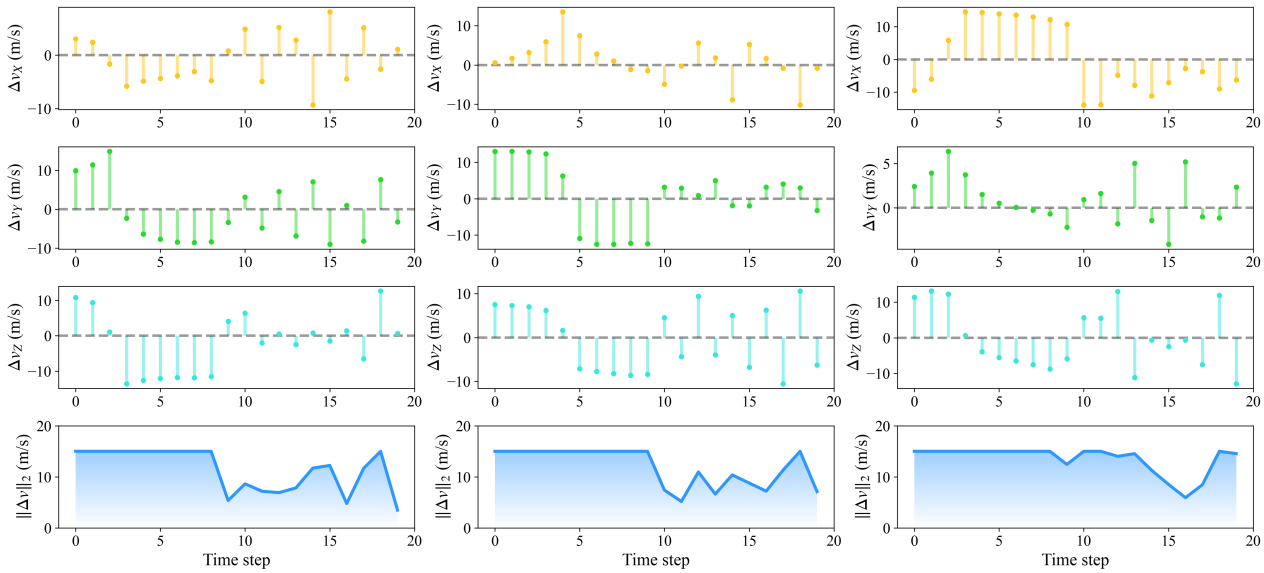

Fig. 4 Interception Control Impulse under MPC with Self-Attention Diffusion Model Prediction

To show the practical value of the proposed online trajectory prediction model, we use the prediction outputs from the DDPM with a self-attention encoder as the noise-fitting network, which has shown

the best prediction performance. These predicted trajectories serve as nominal trajectory references in a model predictive control framework to guide the interceptor spacecraft D for rapid interception of P. In the simulation example, the maximum single impulse of the interceptor spacecraft D is set to 75% of that of spacecraft P. Figure 3 displays the resulting MPC-based interception trajectory that correspond to the typical prediction result shown in Fig. 2. Figure 4 shows the interception impulses executed by D for the three interception trajectories mentioned above. It can be observed that, under the guidance of the predicted trajectories, the interceptor spacecraft effectively accomplished the interception task while satisfying the upper limit constraint on the impulse.

5 Conclusion

In this study, a diffusion-based time-series prediction framework was developed to address the trajectory prediction problem of maneuverable non-cooperative spacecraft whose control laws neither maintain a fixed configuration nor conform to a predefined form. A pursuit–evasion trajectory dataset was constructed in a representative close-range pursuit–evasion game scenario using a reinforcement learning-driven pursuit–evasion strategy that is not explicitly identifiable. The applicability of the Denoising Diffusion Probabilistic Model to non-cooperative spacecraft trajectory forecasting was systematically demonstrated. Numerical simulations validated the effectiveness of the proposed approach and revealed its competitive advantage over other time-series prediction models in terms of prediction accuracy and robustness. Furthermore, the predicted trajectories were successfully integrated into a model predictive control framework to enable precise interception of non-cooperative spacecraft.

The results confirm that the proposed method can serve as a viable solution in space defense applications where traditional configuration classification or parameter identification assumptions are inapplicable. Future work will focus on extending the prediction framework to scenarios involving higher uncertainty, larger maneuver capabilities, and multi-agent interactions, as well as integrating adaptive control strategies to further enhance interception performance under real-world operational constraints.

References

[1] Honglin Zhang, Jianjun Luo, Yuan Gao, and Weihua Ma. An intention inference method for the space non-cooperative target based on BiGRU-Self Attention. *Advances in Space Research*, 72(5):1815–1828, 2023. ISSN: 0273-1177. doi: https://doi.org/10.1016/j.asr.2023.04.032.

[2] Qinbo Sun and Zhaohui Dang. Deep neural network for non-cooperative space target intention recognition. *Aerospace Science and Technology*, 142:108681, 2023. ISSN: 1270-9638. doi: https://doi.org/10.1016/j.ast.2023.108681.

[3] Jiasheng Li, Zhen Yang, and Yazhong Luo. Intention inference for space targets using deep convolutional neural network. *Advances in Space Research*, 75(2):2184–2200, 2025. ISSN: 0273-1177. doi: https://doi.org/10.1016/j.asr.2024.10.006.

[4] Qinbo Sun, Liran Zhao, Shengyong Tang, and Zhaohui Dang. Orbital motion intention recognition for space non-cooperative targets based on incomplete time series data. *Aerospace Science and Technology*, 158:109912, 2025. ISSN: 1270-9638. doi: https://doi.org/10.1016/j.ast.2024.109912.

[5] Xiao Wang, Zhuo Yang, Yuying Han, Hao Li, and Peng Shi. Method of sequential intention inference for a space target based on meta-fuzzy decision tree. *Advances in Space Research*, 74(8):4050–4067, 2024. ISSN: 0273-1177. doi: https://doi.org/10.1016/j.asr.2024.06.049.

[6] Shibo Chen, Jun Li, Yaen Xie, Xiande Wu, Shuhang Leng, and Ruochu Yang. Approaching Intention Prediction of Orbital Maneuver Based on Dynamic Bayesian Network. *Transactions of Nanjing University of Aeronautics & Astronautics*, (4):460–471, 2023. doi: https://doi.org/10.16356/j.1005-1120.2023.04.007.

[7] Zhuo YANG, Peng SHI, Tao ZHOU, and Wen-long LI. Intention recognition method of space non-cooperative target based on fuzzy reasoning. *Journal of Beijing University of Aeronautics and Astronautics*, pages 1–18, 2024.

[8] Ashish Jagat and Andrew J. Sinclair. Optimization Of Spacecraft Pursuit-Evasion Game Trajectories In The Euler-Hill Reference Frame. *AIAA/AAS Astrodynamics Specialist Conference*. doi: 10.2514/6.2014-4131.

[9] Ashish Jagat and Andrew J. Sinclair. Nonlinear Control for Spacecraft Pursuit-Evasion Game Using the State-Dependent Riccati Equation Method. *IEEE Transactions on Aerospace and Electronic Systems*, 53(6):3032–3042, 2017. doi: 10.1109/TAES.2017.2725498.

[10] Mauro Pontani and Bruce A. Conway. Numerical Solution of the Three-Dimensional Orbital Pursuit-Evasion Game. *Journal of Guidance, Control, and Dynamics*, 32(2):474–487, 2009. doi: 10.2514/1.37962.

[11] Dan Shen, Khanh Pham, Erik Blasch, Huimin Chen, and Genshe Chen. Pursuit-Evasion Orbital Game for Satellite Interception and Collision Avoidance. 8044, May 2011. doi: 10.1117/12.882903.

[12] Will Hafer, Helen Reed, James Turner, and Khanh Pham. Sensitivity Methods Applied to Orbital Pursuit Evasion. *Journal of Guidance, Control, and Dynamics*, 38:1–9, Mar. 2015. doi: 10.2514/1.G000832.

[13] Songtao Sun, Qiuhua Zhang, Ryan Loxton, and Bin Li. Numerical solution of a pursuit-evasion differential game involving two spacecraft in low earth orbit. *Journal of Industrial and Management Optimization*, 11:1127–1147, Oct. 2015. doi: 10.3934/jimo.2015.11.1127.

[14] Geng Yuan-Zhuo, Yuan Li, Huang Huang, and Tang Liang. Terminal-guidance based reinforcement-learning for orbital pursuit-evasion game of the spacecraft. *Acta Automatica Sinica*, 49(5):974–984, 2023.

[15] Liran Zhao, Yulin Zhang, and Zhaohui Dang. PRD-MADDPG: An efficient learning-based algorithm for orbital pursuit-evasion game with impulsive maneuvers. *Advances in Space Research*, 72(2):211–230, 2023. ISSN: 0273-1177. doi: https://doi.org/10.1016/j.asr.2023.03.014.

[16] Hongbo Wang and Yao Zhang. Impulsive maneuver strategy for multi-agent orbital pursuit-evasion game under sparse rewards. *Aerospace Science and Technology*, 155:109618, 2024. ISSN: 1270-9638. doi: https://doi.org/10.1016/j.ast.2024.109618.

[17] Zhenyu Li, Hai Zhu, and Yazhong Luo. An escape strategy in orbital pursuit-evasion games with incomplete information. *Science China Technological Sciences*, 64(3):559–570, 2021. ISSN: 1869-1900. doi: 10.1007/s11431-020-1662-0.

[18] Dong Ye, Xu Tang, Zhaowei Sun, and Chunbao Wang. Multiple model adaptive intercept strategy of spacecraft for an incomplete-information game. *Acta Astronautica*, 180:340–349, 2021. ISSN: 0094-5765. doi: https://doi.org/10.1016/j.actaastro.2020.12.015.

[19] Xu Tang, Dong Ye, Lei Huang, Zhaowei Sun, and Jianye Sun. Pursuit-evasion game switching strategies for spacecraft with incomplete-information. *Aerospace Science and Technology*, 119:107–112, 2021. ISSN: 1270-9638. doi: https://doi.org/10.1016/j.ast.2021.107112.

[20] Jonathan Ho, Ajay Jain, and Pieter Abbeel. Denoising diffusion probabilistic models. In *Advances in Neural Information Processing Systems*, volume 33, 2020.

[21] Agathe Girard, Carl Rasmussen, Joaquin Quiñonero Candela, and Roderick Murray-Smith. Gaussian process priors with uncertain inputs application to multiple-step ahead time series forecasting. In *Advances in Neural Information Processing Systems*, volume 15, 2002.